The final publication is available at

https://doi.org/10.1016/j.marpolbul.2019.05.013

Additional Information

1　# Anthropogenic impact on nitrification dynamics in coastal

2　# waters of the Mediterranean Sea

3

4　**Regina Temino-Boes[a],*, Inmaculada Romero[a], María Pachés[a], Remedios Martinez-**

5　**Guijarro[a], Rabindranarth Romero-Lopez[b]**

6

7　a. Instituto de Ingeniería del Agua y del Medio Ambiente, Universitat Politècnica de València, Camino de Vera s/n,

8　Valencia 46022, Spain

9　b. Departamento de Ingeniería Civil, Universidad Veracruzana, Lomas del Estadio s/n, Xalapa 91000, Mexico

10　* Corresponding author

11　**Abstract**

12　The anthropogenic alteration of the nitrogen cycle results in the modification of the whole

13　food web. And yet, the impact caused on nitrogen dynamics in marine systems is still very

14　uncertain. We propose a workflow to evaluate changes to coastal nitrification by modelling

15　nitrite dynamics, the intermediary compound. Nitrite concentrations were estimated with a

16　simple steady state nitrification model, which was calibrated in 9 NW Mediterranean coastal

17　sites with different anthropogenic pressures, located within 250km. The results obtained

18　indicate that nitrite peaks are observed in winter and explained by nitrification response to

19　temperature, but these dynamics are altered in impacted coastal waters. We found the second

20　step of nitrification to be more sensitive to temperature, which entails a significant impact of

21　climate change on the decoupling of the two steps of nitrification. The results could be

22　extrapolated to numerous coastal regions of the Mediterranean Sea with similar

23　characteristics.

24　**Keywords**

25　Nitrification dynamics, Coastal waters, Mediterranean Sea, Anthropogenic impact, Nitrogen

26　cycle, Inorganic Nitrogen Speciation

27　## 1. Introduction

28　　Rockström et al. (2009) established the alteration of the nitrogen (N) cycle as one of the

29　three planetary processes, together with climate change and biodiversity loss, sufficiently

30 altered by human activity as to potentially have disastrous consequences for humans. Some

31 authors are concerned about nitrogen being "the next carbon" (Battye et al., 2017). Due to

32 their vulnerability to anthropogenically driven change, coastal zones have been highly

33 impacted (Arhonditsis et al., 2000; De Vittor et al., 2016; Smith et al., 2014). Population growth

34 and related nutrient sources such as agriculture, wastewater, urban runoff, and fossil fuels

35 have increased nutrient inputs to coastal waters to many times their natural levels (Bricker et

36 al., 2008). As such, many researchers have evidenced the impact that human activities have

37 caused to food webs or biogeochemical processes in many coastal systems (Borja et al., 2004;

38 Lundberg et al., 2005; Wang et al., 1999). In the Mediterranean Sea, direct wastewater

39 discharges account for a large amount of the total nitrogen input (Powley et al., 2016; Stamou

40 and Kamizoulis, 2008). Nearshore coastal waters (0-200 m) are particularly vulnerable and

41 need a special attention, as the nutrient gradient from land to ocean is considerably large in

42 the Mediterranean Sea (Flo et al., 2011).

43   Nitrification plays a crucial role in marine primary production (Yool et al., 2007) and in the N

44 cycle of coastal zones (Damashek et al., 2016; McLaughlin et al., 2017). This process alone does

45 not change the total amount of nitrogen in an ecosystem, but it affects its speciation and fate:

46 nitrate (the product of nitrification) serves as substrate for denitrification, which removes N

47 from the system via N_2 gas (Carini et al., 2010). Nitrification is generally described as a two-

48 step process occurring under aerobic conditions: oxidation of ammonium to nitrite and

49 oxidation of nitrite to nitrate (Kim, 2016). It links reduced and oxidized forms of nitrogen.

50 Although ammonium oxidation is considered the limiting step, both steps are expected to be

51 tightly coupled. However, evidence of decoupling in coastal waters was observed especially at

52 high temperatures (Beman et al., 2013; Heiss and Fulweiler, 2016), which leads to the

53 accumulation of nitrite. As an intermediary compound in many key biological processes, nitrite

54 dynamics have historically been used as an indicator of the balance between oxidative and

55 reductive pathways in marine systems (Lomas and Lipschultz, 2006). Nitrite production

56 processes in aerobic waters include the oxidation of ammonia and assimilatory nitrate

57 reduction by phytoplankton and heterotrophic bacteria, while removal pathways for nitrite

58 include oxidation by nitrite-oxidizing bacteria and phytoplankton uptake (Schaefer and

59 Hollibaugh, 2017).

60   Increasing evidence indicates that many environmental factors such as pH, temperature or

61 oxygen concentration affect nitrification processes (Damashek et al., 2016; Schaefer and

62 Hollibaugh, 2017). However, when it comes to how humans alter inorganic nitrogen

63 transformations in marine environments research is still very scarce. Kim (2016) summarized

64   how climate change will alter marine N cycle and indicated the need for further research on

65   marine inorganic N transformations, while McLaughlin et al (2017) and Bartl et al. (2018)

66   studied the alteration of nitrification caused by wastewater discharges and pointed out the

67   need for further research on anthropogenic nutrient effect on coastal biogeochemistry. Ocean

68   acidification results in reduced nitrification rates (Beman et al., 2010; Huesemann et al., 2002;

69   Kitidis et al., 2011) while other anthropogenic pressures such as N deposition (Kim, 2016) or

70   wastewater effluents might increase nitrification (McLaughlin et al., 2017). Clearly, the overall

71   anthropogenic effect on nitrification in coastal systems needs to be evaluated further. In the

72   Mediterranean Sea, the urbanization on the littoral zone has severely impacted the natural

73   balance of ecosystems (Lejeusne et al., 2010). Nitrification dynamics are altered in those areas

74   with high anthropogenic pressure, leading to a change in nitrogen cycling along the year

75   (Ordines et al., 2015). The modification of such an important process in the N cycle may have

76   consequences on phytoplankton abundance and diversity, with cascading effects on other

77   organisms. The importance of nitrification in the N biogeochemistry in coastal waters has

78   already been proved by many authors (Damashek et al., 2016; Heiss and Fulweiler, 2016;

79   Huesemann et al., 2002), but the mechanisms by which anthropogenic activity alters

80   nitrification in coastal waters need to be studied in more detail.

81   The aim of this study was to propose a simple workflow for the evaluation of nitrification

82   alteration in coastal waters due to anthropogenic activity. Nitrite, as the intermediary

83   compound in the two steps of nitrification, was used to study nitrification. We modelled nitrite

84   dynamics in several coastal sites located within approximately 250 km of coast. All modelled

85   water bodies have similar characteristics but different anthropogenic pressures, so that

86   nitrification parameters could be related to anthropogenic pressure. This methodology is

87   applicable to other coastal areas of the Mediterranean Sea, where nitrification is the main

88   driver of nitrite dynamics (Bianchi et al., 1994).

89   **2. Materials and methods**

90   *2.1. Study area and analytical methods*

91   The Jucar River Basin District (JRBD) lies in the Mediterranean coast of Spain, covering

92   42,735 km^2 with 574 km of coastline. The management plan defines 16 natural coastal water

93   bodies. In this study we focused on 9 of them, which belong to the typology II-A (moderately

94   influenced by freshwater inputs with salinity between 34.5 and 37.5 g Kg^{-1}). These water

95   bodies (presented in Figure 1) have similar geomorphology, littoral transport, dominant winds,

96   rainfall, area of fluvial basins, continental inputs and wet zones. C002 is the reference site for

97　　typology II-A with no relevant anthropogenic influence, as determined by Romero et al. (2013)

98　　and Pachés et al. (2012) who evaluated pressures and impacts according to annex V of the

99　　Water Framework Directive (WFD). Some coastal waters in the JRBD are considered under the

100　　WFD as heavily modified due to the presence of a harbor (Figure 1); these water bodies were

101　　not included in our study.
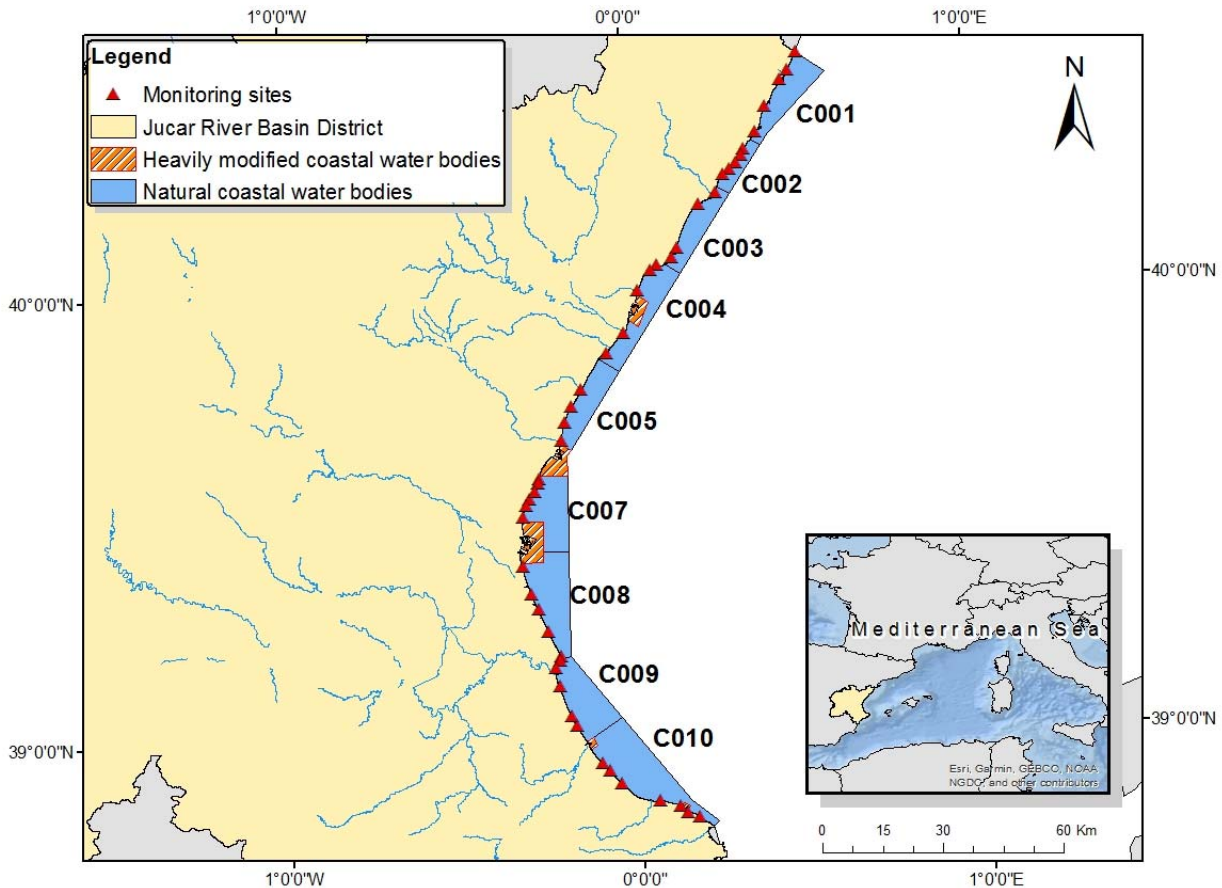
103　　**Figure 1.** Jucar River Basin District: natural coastal water bodies of typology II-A, heavily

104　　modified coastal water bodies ("which as a result of physical alterations by human activity is

105　　substantially changes in character" (European Commission, 2000)) and monitoring sites.

106　　　　Hermosilla Gómez (2009) studied the influence of the sampling locations in the evaluation

107　　of the anthropogenic pressures and the ecological status of the coasts of Valencia. By means of

108　　statistical analysis, she determined that sampling sites should be located inshore (over the

109　　coast) and at the surface so that samples are taken from the area affected by anthropogenic

110　　eutrophication. Besides, the data and methods developed in Spain for the intercalibration

111　　exercise of the Mediterranean intercalibration group (MedGIG) within the WFD are most

112　　based on inshore sampling stations (MedGIG, 2009). Thus, in order to compare the results

113　　obtained in this study with previous ecological evaluations in the water bodies considered,

114   inshore sampling was more convenient. 46 monitoring sites were distributed all along the

115   coast, with 4 to 7 stations in each water body. Each month from August 2008 until January

116   2011, water samples were taken from beyond the wave breakpoint at a 10 cm depth.

117   Temperature was measured in situ with a multiparametric probe YSI (6600 V2).

118   Water samples were collected in plastic bottles, refrigerated, and carried to the laboratory

119   within 12 hours. A Portasal 8410A salinometer was calibrated to determine salinity (I.A.P.S.O.

120   Standard Seawater, Ocean Scientific International Ltd., K15 = 0.99986, S = 34.995‰). Samples

121   were divided into several sets following the conservation procedures suggested by APHA

122   (2005) and filtered through 0.45 μm cellulose acetate membrane filters (Millipore HAWP).

123   These membranes are stored at -20 °C in order to break the cells for chlorophyll-a analysis.

124   For the determination of chlorophyll-a, the trichromatic method was used, based on visible

125   spectroscopy (APHA, 2005). The filters are introduced in 6 ml of 90% acetone in water with 1%

126   calcium carbonate. The optical density of the extract was determined at different wavelengths

127   (630, 647 and 664 nm) to determine the pigment content, and at 750 nm to determine the

128   optical density not due to chlorophyll-a. The equations proposed by Jeffrey and Humprey

129   (1975) were used for concentration calculations. The detection limit was 0.2 mgC.m-3 of

130   chlorophyll-a.

131   Nutrients (ammonium, nitrite and nitrate) were analyzed with an Alliance Instruments

132   Integral Futura air-segmented continuous-flow autoanalyzer, following the procedure

133   described by Treguer and Le Corre (1975) and taking into account the remarks made by

134   Kirkwood et al. (1991) and Parsons et al. (1984). The equipment optimization is carried out

135   following Coakley (1981) theories. Ammonium and nitrite were analyzed with the filtered

136   samples, right after filtration, while the samples kept for nitrate determination were frozen for

137   a later analysis. Ammonium was measured based on Berthelot's reaction. Under alkaline

138   conditions, ammonium reacts with the hypochlorite forming a monochloramine. This

139   compound, in the presence of phenol and an excess of hypochlorite, forms indophenol blue.

140   The nitroprusside ion catalyzes the reaction and trisodium citrate eliminates the interference

141   of Ca and Mg (Solòrzano, 1969). Nitrite concentrations were determined with Shinn (1941)

142   water analysis method, adapted for seawater by Bendschneider and Robinson (1952). This

143   method is based on the reaction of nitrite ion with sulfanilamide in acidic conditions,

144   producing a diazo compound that forms a pink complex with N-naphthylethylene diamine. For

145   the determination of nitrate concentrations, this compound is reduced to nitrite by means of a

146   Cu/Cd reducing column in basic conditions (pH = 8.5), following the method described by

147   (Grasshoff, 1976). Subsequently, nitrite is analyzed by the procedure described above. High

148   purity Merck reagents for analysis and ultra-pure water (Milli-Q 185) were used. The detection

149   limits were 1.4x10-3 mgN.L-1 for ammonium and nitrate and 1.4x10-4 mgN.L-1 for nitrite.

150   *2.2. Workflow*

151   The proposed workflow is schematized in Figure 2 and explained in detail in next sections.
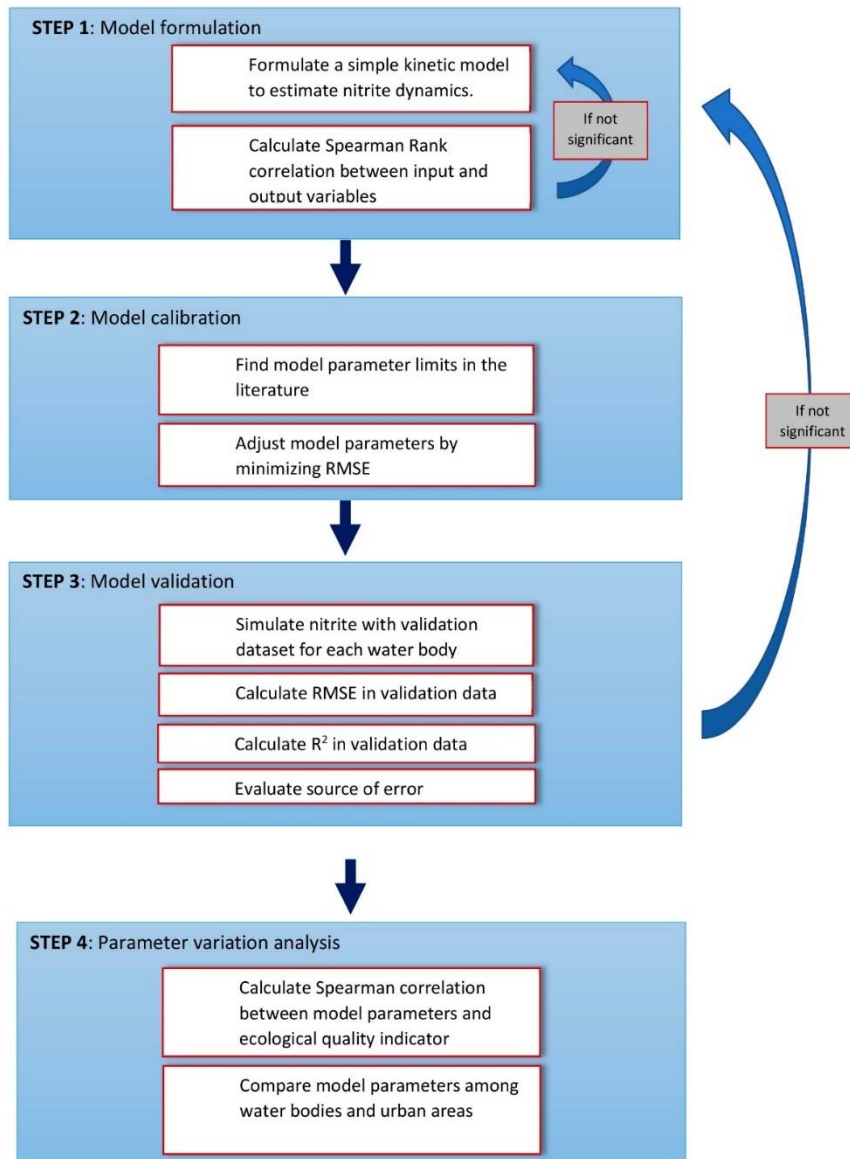
152

153   **Figure 2.** Descriptive diagram of the research workflow

154   *2.2.1. Model formulation*

155   The equation solved is based on the principle of the conservation of mass. The main

156   processes driving nitrite dynamics were studied from the literature and used for the

157   development of the model, neglecting the less relevant processes. We applied a mass balance

158   in zero dimensions in each water body which was considered as a control volume. As samples

159   were taken at the surface, we considered appropriate to neglect the effect of the sediment.

160   Simple and well-known principles can be used to build simple models which can give an overall

161   understanding of nitrogen processes. When a basic understanding of the system is aimed and

162   the requirement to the precision of estimated values is low, simple models perform better

163   (Højberg et al., 2007). Complex models require large amounts of data and such a model would

164   not add value to our research purpose.

165   Nitrite production pathways in coastal waters include ammonia oxidation and assimilatory

166   nitrate reduction by phytoplankton and heterotrophic bacteria, while removal pathways for

167   nitrite include nitrite oxidation and phytoplankton uptake (Schaefer and Hollibaugh, 2017).

168   Ammonium is the preferred form of nitrogen for phytoplankton uptake (Chau and Jin, 1998;

169   Zouiten et al., 2013), so we considered direct nitrite uptake to be negligible. Additionally, the

170   study area is characterized by low phytoplankton concentrations in natural conditions (Pachés

171   et al., 2012). Thus, nitrite release by phytoplankton was also neglected. An analysis of the

172   relationship between the model error and phytoplankton concentrations was carried out to

173   confirm this assumption (see section 2.2.2). Bianchi et al. (1994) also determined that nitrite

174   concentrations in the NW Mediterranean Sea are regulated by the two steps of nitrification.

175   Therefore, we considered only nitrification processes to estimate nitrite: formed with

176   ammonium oxidation (nitrification first step) and eliminated by nitrite oxidation (nitrification

177   second step). Studies carried out in other coastal areas also pointed out the significant role of

178   nitrification (Damashek et al., 2016; Schaefer and Hollibaugh, 2017).

179   At low nitrogen concentrations as those found in natural systems, the process of nitrification

180   is generally represented by a first order kinetic reaction (Bowie et al., 1985). Previous studies

181   typically considered only the temperature effect on nitrification. Some authors also introduced

182   the effect of dissolved oxygen as a limiting factor (Chau and Jin, 1998; Umgiesser et al., 2003;

183   Zouiten et al., 2013). Nonetheless, the samples used in this study, which were taken at the sea

184   surface, had all high oxygen concentrations (averaged 8.3 ± 1.4 mgO.L^{-1} measured during

185   campaigns). Consequently, we did not add oxygen limitation to our model. pH, which also

186   affects nitrification rates (Park et al., 2007), was measured during the campaigns and variations

187   were not relevant (averaged 8.14 ± 0.13).

188   Flo et al. (2011) showed that continental influence is the main driver of nutrient variability

189   within 200m of coast in the NW Mediterranean Sea. The water bodies considered in this study

190   have a length of >13km along the coast, and samples were taken at less than 50m from the

191   coastline. As such, the continental influence on nutrient concentrations is much larger than the

192   effect of the dispersion along the coast. Additionally, as the two steps of nitrification are tightly

193   coupled (Schaefer and Hollibaugh, 2017), nitrite is oxidized to nitrate almost as fast as it is

194   created (see Table 1), whereas longitudinal mixing along >13km is expected to be a much

195   slower process (Stamou and Kamizoulis, 2008). Therefore, we decided not to consider

196   dispersion with adjacent water bodies to simplify our model.

197   The main nitrogen sources to the JRBD coastal waters are agriculture and urban population

198   (Romero et al., 2013), which means that most of the nitrogen inputs are in the form of

199   ammonium or nitrate. Hence, we considered no relevant direct nitrite inputs. An analysis of

200   the relationship between the model error and salinity was carried out to confirm this

201   assumption (see section 2.2.2).

202   Equation 1 represents nitrite mass balance under these assumptions.

203    $$\frac{\partial [NO_2{}^-]}{\partial t} = k_1 \theta_1{}^{T-20} [NH_4{}^+] - k_2 \theta_2{}^{T-20} [NO_2{}^-]$$ Equation 1

204   Where, $[NO_2{}^-]$ is nitrite concentration (mgN.L^{-1}), $[NH_4{}^+]$ is ammonium concentration (mgN.L^{-}

205   ^{1}), t is time (day), k_1 is ammonium oxidation rate at 20°C (day^{-1}), Θ_1 is temperature coefficient

206   for ammonium oxidation, k_2 is nitrite oxidation rate at 20°C (day^{-1}), Θ_2 is temperature

207   coefficient for nitrite oxidation, T is temperature (°C).

208   The steady state approach is very frequently used in water quality modelling (Chapra, 1997;

209   Wang et al., 2013). This approach enables the calculation of the nitrite concentration each

210   month, if the conditions found at the time of the sampling were maintained. Under this

211   assumption the accumulation term was set to zero. Nitrite concentrations can be estimated

212   with the following equation, derived from Equation 1:

213    $$[NO_2{}^-] = \left(\frac{k_1}{k_2}\right)\left(\frac{\theta_1}{\theta_2}\right)^{T-20} [NH_4{}^+]$$ Equation 2

214   K$_1$ and K$_2$ depend mathematically on each other (see K$_1$ and K$_2$ depend mathematically on each

215   other (see Equation 2), making the separate calibration of both parameters unfeasible. The

216   same applied to Θ_1 and Θ_2. We defined K and Θ as new parameters equivalent to the ratios

217   k$_1$/k$_2$ and Θ_1/Θ_2 respectively:

218    $$[NO_2{}^-] = K \cdot \theta^{T-20} [NH_4{}^+]$$ Equation 3

219   Thus, K represents the ratio of ammonium oxidation to nitrite oxidation, while Θ represents

220   the ratio of ammonium to nitrite oxidation sensitivity to temperature.

221   Output sensitivity to input variables can be estimates with Spearman rank correlation

222   coefficient in nonlinear but monotonic relationships (Pianosi et al., 2016). As such, the

223   Spearman correlation coefficient was calculated between selected input (temperature and

224   ammonium) and output variables to determine the relative importance in nitrite estimation.

225   The calculation of this correlation confirms whether the selected input variables are relevant

226   for the estimation of nitrite concentrations, or else the simplified model needs to be re-

227   evaluated.

228   *2.2.2.   Model calibration and validation*

229   We carried out a literature review to set parameter limits. The values found are presented

230   in Table 1.

231   **Table 1**

232   Bibliographical parameter values

Parameter	Range	Unit
K_1	0.05- 0.5	d^{-1}
K_2	0.5 - 10	d^{-1}
Θ_1	1.02 - 1.12	-
Θ_2	1.02 - 1.12	-

233   References: (Bowie et al., 1985; Chau and Jin, 1998; Myszograj, 2015; Zouiten et al., 2013)

234   Mean monthly values for all variables were calculated for each water body from August 2008

235   to January 2011. The dataset was divided in two sub-datasets; one was used as calibration

236   data and the second as validation data. Odd monthly observations (1,3,4…,29) of input and

237   output variables were used for calibration whereas even observations (2,4,6,…,30) were left

238   for validation (see Figure 2). The parameters K and Θ were optimized to reproduce nitrite

239   observed concentrations by minimizing the rooted mean squared error (RMSE) in calibration

240   data. Then, the model was run with the validation dataset and nitrite estimations were

241   compared to observations. The RMSE and the coefficient of determination (R^2) were calculated

242   to estimate the goodness of fit.

243   Two of the neglected processes during the model formulation may be the main source of

244   error to our model: phytoplankton release and continental inputs. To evaluate the source of

245   error in the model, we calculated Spearman correlation between monthly error and

246   phytoplankton and between monthly error and salinity in each water body.

247   *2.2.3. Parameter variation analysis*

248   Once the model was validated, the relationship between model parameter differences

249   among water bodies and two physicochemical variables was evaluated to determine the

250   source of spatial changes in nitrification dynamics. pH and dissolved oxygen were very similar

251   in all water bodies as mentioned above and consequently not included in this evaluation. The

252   two physical variables analyzed were temperature and salinity. The Spearman correlation

253   coefficient between these two variables and calibrated model parameters was calculated to

254   determine whether they may influence the studied nitrification parameter values.

255   Phytoplankton biomass is established as an indicator of the ecological status of coastal

256   waters under the WFD. In the JRBD, Pachés et al. (2012) identified chlorophyll-a 50th percentile

257   to be the most appropriate statistical parameter to measure anthropogenic pressure, and

258   Romero et al. (2013) related phytoplankton to anthropogenic pressures such as population

259   density, agriculture and industry. As such, we used chlorophyll-a 50th percentile as an indicator

260   of the alteration provoked by human pressures. We calculated the Spearman correlation

261   coefficient between model parameters and chlorophyll-a 50th percentile to determine whether

262   anthropogenic pressures may have altered nitrification parameters.

263   **3. Results**

264   *3.1. Variable values*

265   Ammonium, nitrite and nitrate concentrations in each water body are presented in Figure 3, as

266   well as temperature, salinity and chlorophyll-a. The highest N concentrations were found in

267   C007, the water body located north of Valencia city. Chlorophyll-a was also high in C007; the

268   most polluted site of the JRBD (Pachés et al., 2012; Temino-Boes et al., 2018). C002, the

269   reference water body, had low N concentrations, together with C001 and C003. The lowest

270   salinities were found in C005 and C007, with some low salinity events in C009. The latest water

271   body corresponds to the discharge of the Jucar river. Temperature is slightly lower in sites C001

272   to C003.
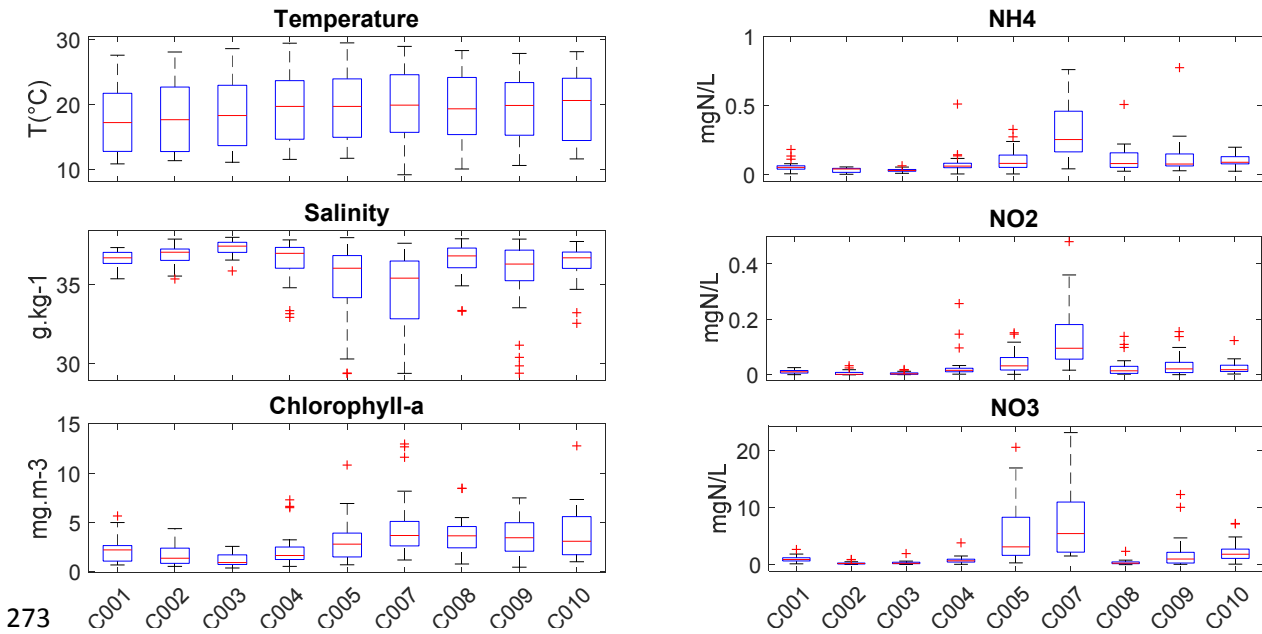
Figure 3. Boxplot of ammonium, nitrite and nitrate concentrations of all water bodies from August 2008 to January 2011. Each data point corresponds to the mean concentration of all monitoring sites of a water body for a given time. Some outliers were also observed in C007 in N concentrations which do not appear in the figure due to the limits of the y-axis.

3.2. Model results

Spearman correlation between model forcings (water temperature and ammonium) and output variable (nitrite concentration) was calculated to determine which variable had the highest influence on nitrite concentrations in each water body. We found a significant rank correlation between nitrite and temperature in all water bodies except C005 and C007 (Table 2) which correspond to the sites with highest continental influence (see salinity in Figure 3). On the other hand, ammonium was significantly correlated to nitrite in all water bodies except C002 to C004. These sites correspond to the lowest observed inorganic nitrogen concentrations and chlorophyll-a (Figure 3).

Table 2

Spearman rank correlation between output variable (nitrite) and input variables (temperature and ammonium)

| Water Body	T (°C)	NH$_4$ (mgN.L^{-1})
C001	-0.38*	0.49*
C002	-0.67*	0.28
C003	-0.55*	0.30
C004	-0.61*	0.44

11

C005	-0.36	0.56*
C007	0.08	0.79*
C008	-0.60*	0.85*
C009	-0.44*	0.57*
C010	-0.37*	0.52*

290   * Significant correlations at the 95% confidence level (p-value < 0.05)

291   We calibrated and validated the model for each water body, and the obtained results are

292   presented in Figure 4. The parameters K and Ө obtained for each water body are shown in

293   Table 3. We calculated the RMSE and R^2 in validation data (Table 3). Ammonium oxidation rate

294   is often estimated as an order of magnitude lower than nitrite oxidation for surface water

295   quality modelling as shown in Table 1. This observation agrees with our findings which

296   established a K mean value of 0.17 (Table 3).

297   In most water bodies Ө was below 1, which indicates that nitrite oxidation is more sensitive

298   to temperature changes than ammonium. Under this circumstance, nitrite peaks are observed

299   in low temperature periods (December and January). The sites with the lowest anthropogenic

300   pressures (C002 and C003) show clear nitrite peaks in the mentioned period. Only two water

301   bodies (C007 and C008) presented a Ө higher than 1.
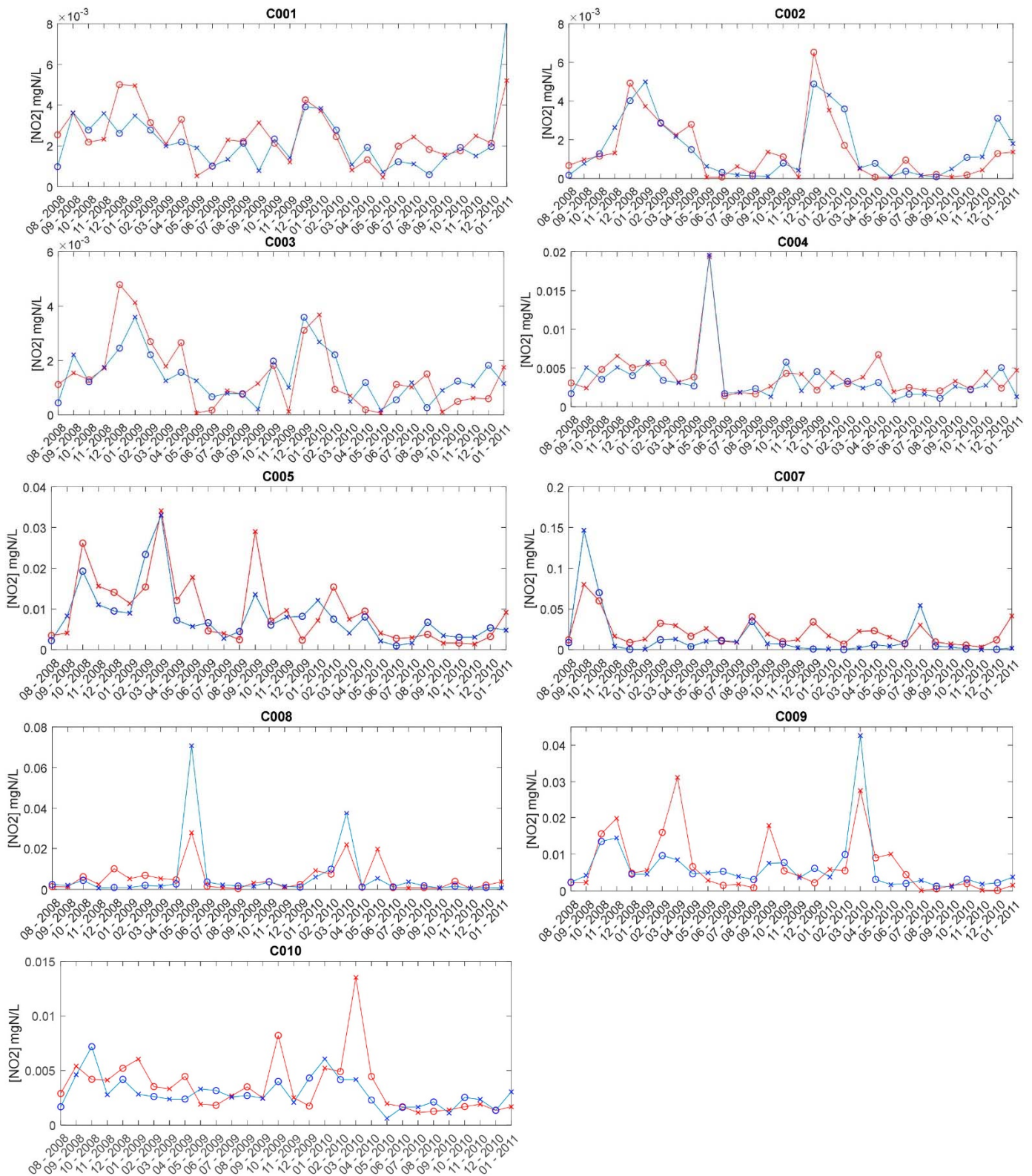
303 **Figure 4.** Mean nitrite measured (red line) and estimated (blue line) concentrations in all water
304 bodies from August 2008 to January 2011.

13

305 **Table 3**

306 Calibrated parameters (K and Θ) for each water body, root mean squared error (RMSE) and

307 coefficient of determination (R^2) between measured and estimated nitrite concentration in

308 validation data

Water body	K	Θ	RMSE (mgN.L^{-1})	R^2
C001	0.15	0.94	1.33E-03	0.55*
C002	0.08	0.80	7.10E-04	0.84*
C003	0.13	0.91	6.75E-04	0.71*
C004	0.20	0.98	1.49E-03	0.95*
C005	0.33	0.92	5.97E-03	0.70*
C007	0.09	1.27	2.46E-02	0.74*
C008	0.11	1.10	1.30E-02	0.72*
C009	0.25	0.97	8.37E-03	0.46*
C010	0.19	0.97	2.61E-03	0.31*

309 * Significant correlations at the 95% confidence level (p-value < 0.05)

310 No significant correlation was found in any water body between monthly error and

311 chlorophyll-a (as a measure of phytoplankton), while the correlation with salinity was

312 significant in water bodies C005 and C010 (Table 4). When salinity was low, the model error

313 was higher due to continental nitrite inputs which were not considered in the model.

314 **Table 4**

315 Spearman rank correlation between error with chlorophyll-a (Chl-a) and salinity (S)

Water Body	S	Chl-a
C001	-0.27	-0.06
C002	-0.26	-0.11
C003	0.15	0.01
C004	0.34	0.29
C005	0.52*	-0.16
C007	0.34	0.26
C008	0.03	-0.09
C009	0.48*	-0.22
C010	0.33	-0.05

316 * Significant correlations at the 95% confidence level (p-value < 0.05)

317 *3.3. Analysis of spatial parameter variations*

318   Spearman rank correlations between salinity, temperature and chlorophyll-a with model

319   parameters and RMSE are calculated in Table 5. Both Ө and the RMSE have a high rank

320   correlation with chlorophyll-a 50th percentile, an indicator of the ecological status of coastal

321   waters. Additionally, salinity is related to the RMSE.

322   **Table 5**

323   Spearman Rank Correlation of model parameters and root mean squared error (RMSE) with

324   mean salinity, mean temperature and chlorophyll-a 50th percentile.

	Salinity (g.kg^{-1})	Temperature (°C)	P50 Chlorophyll-a
K	-0.41	0.45	0.02
Ө	-0.42	0.50	0.80*
RMSE	-0.73*	0.42	0.97*

325   Note: Significant correlations at the 95% confidence level (p-value < 0.05) are marked with an

326   asterisk

327   Figure 5 shows how the parameter Ө, which represents the difference in temperature

328   influence between ammonium and nitrite oxidation, is influenced by anthropogenic activity.

329   Closer to big urban areas, like the city of Valencia in C007, Ө increases, while it decreases in

330   C002 or C003 where the population is smaller. On the contrary, K does not have an

331   anthropogenic influence (*Table 5*).

332
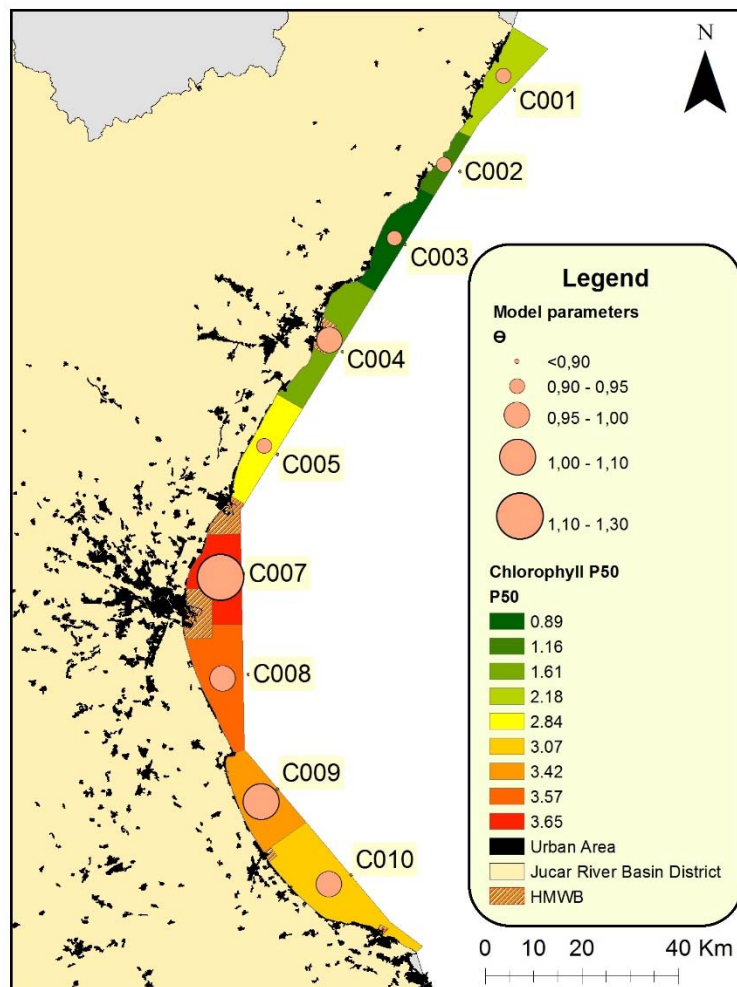
Figure 5. Model parameter Ɵ for each water body, 50th percentile of chlorophyll-a, population
and Heavily modified water bodies (HMWB) due to the presence of a harbour.

4. Discussion

The natural annual cycle of nitrite showed peaks in cold months (December and January), as
found in the reference water body C002 (Figure 4). However, this cycle was highly perturbed in
anthropogenically altered coastal zones, with peaks occurring both in cold and warm seasons
driven by ammonium concentrations. Our results demonstrate that the two steps of
nitrification are decoupled in coastal waters, agreeing with late findings (Heiss and Fulweiler,
2016; Schaefer and Hollibaugh, 2017). Different speeds in the two steps of nitrification were
also observed in the Jucar estuary (Romero et al., 2007). In our model, peaks occur due to the
different response to temperature in ammonium and nitrite oxidation (parameter Ɵ). Many
previous studies found high nitrite concentrations at warmer seasons (Bristow et al., 2015;

16

345 Heiss and Fulweiler, 2016; Schaefer and Hollibaugh, 2017) while others (such as this study)

346 observed nitrite peaks at low temperatures (Pitcher et al., 2011).

347 The changes observed in nitrite dynamics among water bodies indicate a shift in nitrification

348 temperature dependence parameter Θ due to anthropogenic activity (Figure 5). Nitrification

349 requires the mediation of a vast diversity of microorganisms, which makes it an essential

350 process for marine life. Pachés et al. (2012) proved how anthropogenic activity is changing

351 microorganism composition in coastal waters of the JRBD, which may explain the spatial

352 differences found in ammonium and nitrite oxidation temperature parameters. Although no

353 previous study considered this dependence in coastal waters, studies carried out in

354 wastewater determined the dependence of nitrification temperature coefficient on

355 microorganism composition and abundance (Myszograj, 2015). In addition, wastewater

356 effluents alter the biogeochemical cycling and phytoplankton composition (Howard et al.,

357 2017) which may have caused shifts in nitrification temperature dependence. Future research

358 is required to describe the processes driving nitrification dependency on temperature.

359 Previous studies identified a dependence of nitrification rates on salinity (Bernhard et al.,

360 2007; Heiss and Fulweiler, 2016), and low salinity events with elevated concentrations of

361 certain ammonium oxidizing archaea (Schaefer and Hollibaugh, 2017). Bernhard et al. (2005)

362 indicated that the abundance and diversity of ammonium oxidizing bacteria is highly controlled

363 by salinity, and Heiss and Fulweiler (2016) found lower nitrite oxidation rates with higher

364 salinity events. Bianchi et al. (1999) linked high ammonium oxidizing rates with low salinity

365 events in the NW Mediterranean Sea.

366 We found temperature to be an important driver of ammonium and nitrite oxidation

367 decoupling under natural conditions, which entails climate change could have a great impact in

368 this process. In the reference water body C002, which represents unaltered nutrient

369 concentrations, the value of Θ was lower than 1. This result indicates that under pristine

370 conditions the second step of nitrification (nitrite oxidation) is more sensitive to temperature

371 than the first step. Climate change will therefore have a greater impact in this second step. In

372 addition, some studies forecast an important precipitation loss in the Jucar area (Chirivella et

373 al., 2016; Miró et al., 2018) which would considerably reduce the riverine inputs of ammonium

374 and other forms of nitrogen. The decrease in ammonium concentrations would have a direct

375 effect on the rate of nitrification. Therefore, it may be expected to have lower nitrite

376 concentrations due to reduced nitrification rates and a shift in nitrite peaks due to higher

377 temperatures. Further research is needed to evaluate how the combined effect of nitrogen

378 pollution and climate change will modify the nitrification process in coastal waters.

17

379   The model performed well in general. However, there was a wide variation among sites in

380   the accuracy of the model. The coefficient of determination R^2 is lower in C001, C009 and C010

381   (Table 3). As the number of stressors increases, the functioning of the ecosystem is altered,

382   and the estimation of nutrient concentrations is hindered (O'Meara et al., 2017). High nitrite

383   events no longer occur due to natural conditions but rather to an unusual increase in human

384   inputs. Continental inputs are the main source of error to sites C005 and C009 as shown by the

385   Spearman correlations between error and salinity (see Table 4). Those water bodies have

386   higher continental influence as indicated by the low salinities. The Jucar river discharges in

387   C009, which is most probably the source of nitrite during the peaks not reproduced by the

388   model. High nitrite concentrations in C010 also correspond to low salinity event indicating an

389   external source of nitrite not simulated in our model. Although nitrite concentrations in C001

390   did not have a significant correlation with salinity, this water body is located close to the Ebro

391   delta, which may influence nitrification dynamics in this water body. On the other hand,

392   phytoplankton does not have a significant correlation with the error (Table 4) which indicates

393   that neglecting phytoplankton uptake and release is not an important source of error to the

394   model.

395   The proposed workflow is applicable to other coastal areas with samples taken at the surface

396   to avoid the effect of dissolved oxygen limitation. pH variations along the year in the

397   Mediterranean Sea are usually less than ± 0.1 pH units (Flecha et al., 2015), and therefore pH is

398   not expected to be one of the main drivers of nitrification. The effect of phytoplankton and

399   external inputs are the most important processes to be considered before applying the model

400   to other coastal areas. In the Mediterranean Sea, marine waters are often oligotrophic

401   (Vollenweider et al., 1996) and phytoplankton release of nitrite is presumably negligible in

402   most areas. The nitrification kinetic model proposed could be extended to add other processes

403   in the application to other study sites. However, the steps proposed in the workflow of Figure

404   2 can be followed for the study of any areas if the model is adapted. Future studies are needed

405   to evaluate the mechanisms by which nitrification dynamics are altered by human activity and

406   which are its most relevant consequences.

407   **5. Conclusions**

408   Our results show how nitrification dynamics are perturbed in highly populated coastal zones.

409   Under natural conditions nitrite peaks are observed in winter due to low temperatures, but

410   this tendency is completely altered in anthropogenically impacted water bodies. The change

411   observed in the sensitivity to temperature of the two steps of nitrification was highly

18

412 correlated to chlorophyll-a 50th percentile, a measure of the ecological status (Spearman

413 correlation r=0.80). Temperature was the main driver of monthly variation in natural

414 conditions, which indicates a potential effect of climate change on nitrification dynamics.

415 Nitrification is a fundamental process of nitrogen biogeochemistry. As a key nutrient, the

416 alteration of the nitrogen cycle may result in the change of the whole food web in marine

417 ecosystems. Further research concerning the human driven changes of the nitrogen cycle in

418 marine environments is essential to enable experts to propose recovery measures and avoid

419 reaching a point of no return.

425 **References**

426 APHA, 2005. Standard Methods for the Examination of Water and Wastewater, 21th ed.

427 American Public Health Association, American Water Works Association, Water

428 Environment Federation, Washington D.C.

429 Arhonditsis, G., Tsirtsis, G., Angelidis, M.O., Karydis, M., 2000. Quantification of the effects of

430 nonpoint nutrient sources to coastal marine eutrophication: applications to a semi-

431 enclosed gulf in the Mediterranean Sea. Ecol. Modell. 129, 209–227. doi:10.1016/S0304-

432 3800(00)00239-8

433 Bartl, I., Liskow, I., Schulz, K., Umlauf, L., Voss, M., 2018. River plume and bottom boundary

434 layer – Hotspots for nitrification in a coastal bay? Estuar. Coast. Shelf Sci. 208, 70–82.

435 doi:10.1016/J.ECSS.2018.04.023

436 Battye, W., Aneja, V.P., Schlesinger, W.H., 2017. Is nitrogen the next carbon? Earth's Futur. 5,

437 894–904. doi:10.1002/2017EF000592

438 Beman, J.M., Chow, C.E., King, A.L., Feng, Y., Fuhrman, J.A., Andersson, A., Bates, N.R., Popp,

439 B.N., Hutchins, D.A., 2010. Global declines in oceanic nitrification rates as a consequence

440 of ocean acidification 108, 208–213. doi:10.1073/pnas.1011053108

441 Beman, J.M., Leilei Shih, J., Popp, B.N., 2013. Nitrite oxidation in the upper water column and
442   oxygen minimum zone of the eastern tropical North Pacific Ocean. ISME J. 7, 2192–2205.
443   doi:10.1038/ismej.2013.96

444 Bendschneider, K., Robinson, R.J., 1952. A new spectrophotometric determination of nitrite in
445   sea water. J. Mar. Res. 2, 87–96.

446 Bernhard, A.E., Donn, T., Giblin, A.E., Stahl, D.A., 2005. Loss of diversity of ammonia-oxidizing
447   bacteria correlates with increasing salinity in an estuary system. Environ. Microbiol. 7,
448   1289–1297. doi:10.1111/j.1462-2920.2005.00808.x

449 Bernhard, A.E., Tucker, J., Giblin, A.E., Stahl, D.A., 2007. Functionally distinct communities of
450   ammonia-oxidizing bacteria along an estuarine salinity gradient. Environ. Microbiol. 9,
451   1439–1447. doi:10.1111/j.1462-2920.2007.01260.x

452 Bianchi, M., Feliatra, Lefevre, D., 1999. Regulation of nitrification in the land-ocean contact
453   area of the Rhône River plume (NW Mediterranean). Aquat. Microb. Ecol. 18, 301–312.
454   doi:10.3354/ame018301

455 Bianchi, M., Morin, P., Le Corre, P., 1994. Nitrification rates, nitrite and nitrate distribution in
456   the Almeria-Oran frontal systems (eastern Alboran Sea). J. Mar. Syst. 5, 327–342.
457   doi:10.1016/0924-7963(94)90054-X

458 Borja, Á., Franco, J., Valencia, V., Bald, J., Muxika, I., Belzunce, M.J., Solaun, O., 2004.
459   Implementation of the European water framework directive from the Basque country
460   (northern Spain): a methodological approach. Mar. Pollut. Bull. 48, 209–218.
461   doi:10.1016/j.marpolbul.2003.12.001

462 Bowie, G.L., Mills, W.B., Porcella, D.B., Campbell, C.L., Pagenkopf, J.R., Rupp, G.L., Johnson,
463   K.M., Chan, P.W.H., Gherini, S.A., 1985. Rates, Constants, and Kinetics Formulations in
464   Surface Water Quality Modeling (Second Edition). U.S. Environ. Prot. Agency.

465 Bricker, S.B., Longstaff, B., W., D., Jones, A., Boicourt, K., Wicks, C., Woerner, J., 2008. Effects of
466   nutrient enrichment in the nation's estuaries: A decade of change. Harmful Algae 8, 21–
467   32.

468 Bristow, L.A., Sarode, N., Cartee, J., Caro-Quintero, A., Thamdrup, B., Stewart, F.J., 2015.
469   Biogeochemical and metagenomic analysis of nitrite accumulation in the Gulf of Mexico

470   hypoxic zone. Limnolo. doi:10.1002/lno.10130

471   Carini, S.A., McCarthy, M.J., Gardner, W.S., 2010. An isotope dilution method to measure

472   nitrification rates in the northern Gulf of Mexico and other eutrophic waters. Cont. Shelf

473   Res. 30, 1795–1801.

474   Chapra, S.C., 1997. Surface Water Quality Modelling. New York.

475   Chau, K.W., Jin, H., 1998. Eutrophication Model for a Coastal Bay in Hong Kong. J. Environ. Eng.

476   124, 628–638. doi:10.1061/(ASCE)0733-9372(1998)124:7(628)

477   Chirivella, V., Capilla, J.E., Pérez-Martín, M.A., 2016. Dynamical versus statistical downscaling

478   for the generation of regional climate change scenarios at a Western Mediterranean

479   basin: The Júcar River District. J. Water Clim. Chang. 7, 379–392.

480   doi:10.2166/wcc.2015.207

481   Coakley, W.A., 1981. Handbook of automated analysis. Continuous flow techniques. Marcel

482   Dekker, New York.

483   Damashek, J., Casciotti, K.L., Francis, C.A., 2016. Variable Nitrification Rates Across

484   Environmental Gradients in Turbid, Nutrient-Rich Estuary Waters of San Francisco Bay.

485   Estuaries and Coasts 39, 1050–1071. doi:10.1007/s12237-016-0071-7

486   De Vittor, C., Relitti, F., Kralj, M., Covelli, S., Emili, A., 2016. Oxygen, carbon, and nutrient

487   exchanges at the sediment-water interface in the Mar Piccolo of Taranto (Ionian Sea,

488   southern Italy). Environ. Sci. Pollut. Res. 23, 12566–12581. doi:10.1007/s11356-015-

489   4999-0

490   European Commission, 2000. Directive 2000/60/EC of the European Parliament and of the

491   Council of 23 October 2000 establishing a framework for Community action in the field of

492   water policy.

493   Flecha, S., Pérez, F.F., García-Lafuente, J., Sammartino, S., Ríos, A.F., Huertas, I.E., 2015. Trends

494   of pH decrease in the Mediterranean Sea through high frequency observational data:

495   indication of ocean acidification in the basin. J. Chem. Inf. Model. 53, 1689–1699.

496   doi:10.10138/srep16770

497   Flo, E., Garcés, E., Manzanera, M., Camp, J., 2011. Coastal inshore waters in the NW

498   Mediterranean: Physicochemical and biological characterization and management

499   implications. Estuar. Coast. Shelf Sci. 93, 279–289. doi:10.1016/j.ecss.2011.04.002

500   Grasshoff, K., 1976. Methods of seawater analysis. Verlag Chemie: Weinstein, New York.

501   Heiss, E.M., Fulweiler, R.W., 2016. Coastal water column ammonium and nitrite oxidation are
502   decoupled in summer. Estuar. Coast. Shelf Sci. 178, 110–119.
503   doi:10.1016/J.ECSS.2016.06.002

504   Hermosilla Gómez, Z., 2009. Desarrollo metodológico para la correcta evaluación del estado
505   ecológico de las aguas costeras de la Comunidad Valenciana, en el ámbito de la Directiva
506   Marco del Agua, utilizando la clorofila a como parámetro indicador de la calidad.
507   Universitat Politècnica de València.

508   Højberg, A.L., Refsgaard, J.C., Van Geer, F., Jørgensen, L.F., Zsuffa, I., 2007. Use of Models to
509   Support the Monitoring Requirements in the Water Framework Directive. Water Resour.
510   Manag. 21, 1649–1672. doi:10.1007/s11269-006-9119-y

511   Howard, M.D.A., Kudela, R.M., McLaughlin, K., 2017. New insights into impacts of
512   anthropogenic nutrients on urban ecosystem processes on the Southern California
513   coastal shelf: Introduction and synthesis. Estuar. Coast. Shelf Sci. 186, 163–170.
514   doi:10.1016/J.ECSS.2016.06.028

515   Huesemann, M.H., Skillman, A.D., Crecelius, E.A., 2002. The inhibition of marine nitrification by
516   ocean disposal of carbon dioxide. Mar. Pollut. Bull. 44, 142–148. doi:10.1016/S0025-
517   326X(01)00194-1

518   Jeffrey, S.W., Humprey, G.F., 1975. New spectrophotometric equations for determining
519   chlorophylls a, b, and c in higher plants, algae and natural phytoplankton. Biochem. und
520   Physiol. der Pflanz. 167, 191–194.

521   Kim, H., 2016. Review of inorganic nitrogen transformations and effect of global climate
522   change on inorganic nitrogen cycling in ocean ecosystems. Ocean Sci. J. 51, 159–167.
523   doi:10.1007/s12601-016-0014-z

524   Kirkwood, D., Aminot, A., Pertillä, M., 1991. Report on the Results of the ICES Fourth
525   Intercomparison Exercise for Nutrients in Sea Water. Cooperative Research Report No.
526   174, International Council for the Exploration of the Sea. Copenhagen.

527   Kitidis, V., Laverock, B., McNeill, L.C., Beesley, A., Cummings, D., Tait, K., Osborn, M.A.,

528 Widdicombe, S., 2011. Impact of ocean acidification on benthic and water column

529 ammonia oxidation. Geophys. Res. Lett. 38, 2–6. doi:10.1029/2011GL049095

530 Lejeusne, C., Chevaldonné, P., Pergent-Martini, C., Boudouresque, C.F., Pérez, T., 2010. Climate

531 change effects on a miniature ocean: the highly diverse, highly impacted Mediterranean

532 Sea. Trends Ecol. Evol. 25, 250–260. doi:10.1016/j.tree.2009.10.009

533 Lomas, M.W., Lipschultz, F., 2006. Forming the primary nitrite maximum: Nitrifiers or

534 phytoplankton? Limnol. Oceanogr. 51, 2453–2467. doi:10.4319/lo.2006.51.5.2453

535 Lundberg, C., Lönnroth, M., Von Numers, M., Bonsdorff, E., 2005. A multivariate assessment of

536 coastal eutrophication. Examples from the Gulf of Finland, northern Baltic Sea. Mar.

537 Pollut. Bull. 50, 1185–1196. doi:10.1016/j.marpolbul.2005.04.029

538 McLaughlin, K., Nezlin, N.P., Howard, M.D.A., Beck, C.D.A., Kudela, R.M., Mengel, M.J.,

539 Robertson, G.L., 2017. Rapid nitrification of wastewater ammonium near coastal ocean

540 outfalls, Southern California, USA. Estuar. Coast. Shelf Sci. 186, 263–275.

541 doi:10.1016/J.ECSS.2016.05.013

542 MedGIG, 2009. Water Framework Directive inercalibration technical report. Part 3: Coastal and

543 Transitional waters.

544 Miró, J.J., Estrela, M.J., Caselles, V., Gómez, I., 2018. Spatial and temporal rainfall changes in

545 the Júcar and Segura basins (1955–2016): Fine-scale trends. Int. J. Climatol. 38, 4699–

546 4722. doi:10.1002/joc.5689

547 Myszograj, S., 2015. The Impact of Temperature on the Removal of Nitrogen Compounds in

548 Activated Sludge System. Br. J. Appl. Sci. Technol. 11, 1–13.

549 doi:10.9734/BJAST/2015/18950

550 O'Meara, T.A., Hillman, J.R., Thrush, S.F., 2017. Rising tides, cumulative impacts and cascading

551 changes to estuarine ecosystem functions. Sci. Rep. 7, 1–7. doi:10.1038/s41598-017-

552 11058-7

553 Ordines, F., Farriols, M.T., Lleonart, J., Guijarro, B., Quetglas, A., Massutí, E., SCOULLOS, M.,

554 2015. Biology and population dynamics of by-catch fish species of the bottom trawl

555 fishery in the western Mediterranean, Mediterranean Marine Science. Hellenic Center for

556 Marine Research.

557   Pachés, M., Romero, I., Hermosilla, Z., Martinez-Guijarro, R., 2012. PHYMED: An ecological

558   classification system for the Water Framework Directive based on phytoplankton

559   community composition. Ecol. Indic. doi:10.1016/j.ecolind.2011.07.003

560   Park, S., Bae, W., Chung, J., Baek, S.C., 2007. Empirical model of the pH dependence of the

561   maximum specific nitrification rate. Process Biochem. 42, 1671–1676.

562   doi:10.1016/j.procbio.2007.09.010

563   Parsons, T.R., Maita, Y., Lalli, C.M., 1984. A Manual of Chemical and Biological Methods for

564   Seawater Analysis. Pergamon Press, London.

565   Pianosi, F., Beven, K., Freer, J., Hall, J.W., Rougier, J., Stephenson, D.B., Wagener, T., 2016.

566   Sensitivity analysis of environmental models: A systematic review with practical

567   workflow. Environ. Model. Softw. 79, 214–232. doi:10.1016/J.ENVSOFT.2016.02.008

568   Pitcher, A., Wuchter, C., Siedenberg, K., Schouten, S., Damsté, J.S.S., 2011. Crenarchaeol tracks

569   winter blooms of ammonia-oxidizing Thaumarchaeota in the coastal North Sea. Limnol.

570   Oceanogr. 56, 2308–2318. doi:10.4319/lo.2011.56.6.2308

571   Powley, H.R., Du, H.H., Lima, A.T., Krom, M.D., Cappellen, P. Van, 2016. Direct Discharges of

572   Domestic Wastewater are a Major Source of Phosphorus and Nitrogen to the

573   Mediterranean Sea. Environ. Sci. Technol. 50, 8722–8730. doi:10.1021/acs.est.6b01742

574   Rockström, J., Steffen, W., Noone, K., Persson, Å., Chapin, F.S., Lambin, E.F., Lenton, T.M.,

575   Scheffer, M., Folke, C., Schellnhuber, H.J., Nykvist, B., de Wit, C.A., Hughes, T., van der

576   Leeuw, S., Rodhe, H., Sörlin, S., Snyder, P.K., Costanza, R., Svedin, U., Falkenmark, M.,

577   Karlberg, L., Corell, R.W., Fabry, V.J., Hansen, J., Walker, B., Liverman, D., Richardson, K.,

578   Crutzen, P., Foley, J.A., 2009. A safe operating space for humanity. Nature 461, 472–475.

579   doi:10.1038/461472a

580   Romero, I., Moragues, M., González del Río, J., Hermosilla, Z., Sánchez-Arcilla, A., Sierra, J.P.,

581   Mösso, C., 2007. Nutrient Behavior in the Júcar Estuary and Plume. J. Coast. Res. Spec.

582   Issue 48 – 55.

583   Romero, I., Pachés, M., Martínez-Guijarro, R., Ferrer, J., 2013. Glophymed: An index to

584   establish the ecological status for the Water Framework Directive based on

585   phytoplankton in coastal waters. Mar. Pollut. Bull. 75, 218–223.

586   doi:10.1016/j.marpolbul.2013.07.028

587 Schaefer, S.C., Hollibaugh, J.T., 2017. Temperature Decouples Ammonium and Nitrite
588   Oxidation in Coastal Waters. Environ. Sci. Technol. 51, 3157–3164.
589   doi:10.1021/acs.est.6b03483

590 Shinn, M.B., 1941. Colorimetric method for the determination of nitrite. Ind. Eng. Chem. Anal.
591   Ed. 13, 33–35.

592 Smith, A.F., Fryer, R.J., Webster, L., Berx, B., Taylor, A., Walsham, P., Turrell, W.R., 2014.
593   Setting background nutrient levels for coastal waters with oceanic influences. Estuar.
594   Coast. Shelf Sci. 145, 69–79. doi:10.1016/j.ecss.2014.04.006

595 Solòrzano, L., 1969. Determination of ammonia in natural waters by the phenol hypoclorite
596   method. Limnol. Oceanogr. 14, 799–801.

597 Stamou, A.I., Kamizoulis, G., 2008. Estimation of the effect of the degree of sewage treatment
598   on the status of pollution along the coastline of the Mediterranean Sea using broad scale
599   modelling. J. Environ. Manage. 90, 931–939. doi:10.1016/j.jenvman.2008.02.008

600 Temino-Boes, R., Romero, I., Martinez-Guijarro, R., Pachés, M., 2018. The importance of
601   considering pollution along the coast from heavily modified water bodies under the
602   water framework directive. WIT Trans. Ecol. Environ. 228, 307–316.
603   doi:10.2495/WP180291

604 Treguer, P., Le Corre, P., 1975. Manuel d'analyse des sels nutritifs dans l'eau de mer, Brest:
605   Université de Bretagne Occidentale.

606 Umgiesser, G., Melaku Canu, D., Solidoro, C., Ambrose, R., 2003. A finite element ecological
607   model: a first application to the Venice Lagoon. Environ. Model. Softw. 18, 131–145.
608   doi:10.1016/S1364-8152(02)00056-7

609 Vollenweider, R.., Rinaldi, A., Viviani, R., Todini, E., 1996. Assessment of the state of
610   eutrophication in the Mediterranean Sea. Technical Reports Series No . 106. Athens.

611 Wang, P.F., Martin, J., Morrison, G., 1999. Water Quality and Eutrophication in Tampa Bay,
612   Florida. Estuar. Coast. Shelf Sci. 49, 1–20. doi:http://dx.doi.org/10.1006/ecss.1999.0490

613 Wang, Q., Li, S., Jia, P., Qi, C., Ding, F., 2013. A review of surface water quality models.
614   ScientificWorldJournal. 2013, 231768. doi:10.1155/2013/231768

615   Yool, A., Martin, A.P., Fernández, C., Clark, D.R., 2007. The significance of nitrification for

616   oceanic new production. Nature 447, 999–1002. doi:10.1038/nature05885

617   Zouiten, H., Díaz, C.Á., Gómez, A.G., Cortezón, J.A.R., Alba, J.G., 2013. An advanced tool for

618   eutrophication modeling in coastal lagoons: Application to the Victoria lagoon in the

619   north of Spain. Ecol. Modell. 265, 99–113. doi:10.1016/j.ecolmodel.2013.06.009

620